Simulation Study on Aerodynamic Characteristics of Combined Low Aspect Ratio UAV

Yunlong Li[1,2], Xiaoping Xu[1,2], Zhou Zhou[1,2], Yu Bai[1,2], Han Wang[1,2]&Binzhuo Xu[1,2]

[1] School of Aeronautics, Northwestern Polytechnical University, Xi'an 710072, China
[2] National Key Laboratory of Aircraft Configuration Design, Xi'an 710072, China

Abstract

Combined unmanned aerial vehicle (UAV) is a kind of new concept aircraft, which is composed of several small UAVs connected by their wingtips. It has both the high-aspect ratio aircraft's high-altitude and long endurance capability and the distributed mission utility of cluster UAV, and has great development potential. In this paper, a high-fidelity numerical simulation method for multi-body combined UAV based on unstructured polyhedral mesh is established, and the accuracy of the calculation method is verified by a standard example. Firstly, a low aspect ratio UAV configuration suitable for cluster combat is designed. Secondly, the lift-drag characteristics, longitudinal static stability and flow separation characteristics of the combination and each element are analyzed. Finally, the coupling mechanism of wingtip vortex induced drag and wing surface pressure differential drag in low aspect ratio configuration is explored. The results show that the wingtip connection can significantly improve the cruise lift-drag ratio of UAVs with low aspect ratio, and the increment of cruise lift-drag ratio and longitudinal static stability margin gradually decreases with the increase of the number of connections. The swept wing configuration combination is separated at a smaller angle of attack, while the flat wing and forward swept wing configuration combination have stronger drag to flow separation. The low aspect ratio configuration is significantly affected by the coupling effect of wingtip vorticity induced drag and wing surface pressure differential drag. Only when the wingtips of five or more UAVs with low aspect ratio are connected, the drag coefficient of the combination is smaller than that of the single one.

Keywords: Aerodynamic layout; Combined UAV; Low aspect ratio; Wingtip vortex; Flow separation

1. Introduction

The concept of Unmanned Aerial Vehicle cluster combat has been proposed in recent years. A large number of small UAVs rely solely on local perception and simple rules to achieve task coordination, overall behavior emergence, and take the initiative in confronting with numerical advantage [1-2]. However, due to the relatively low aspect ratio of the unit UAV in the UAV cluster, it is significantly affected by wingtip vortex downwash flow, resulting in insufficient navigation time and range for the unit UAV as well as weak platform load capacity, which greatly limits the performance of the cluster. In contrast, Combined UAV is a new concept aircraft formed by combining multiple fixed-wing UAVs at

wingtips or other positions. The combination forms include but are not limited to parallel wingtip parallel combination, flat network combination etc. while connection forms include but are not limited to rigid connection, articulated connection or flexible connection [3-4]. The combined UAV can be designed as a combination of multiple low aspect ratio UAVs that retains high-altitude and long-endurance capability like high-aspect ratio UAV while also possessing distributed mission utility and low-cost economic advantages like cluster UAV with great development potential [5-7].

The concept of combined UAV first appeared in 1931. Based on the F9C-2 "Falcon" combat reconnaissance aircraft, the US Navy combined the wing hook with the airship to form a separable recovery combination [8]. In the 1940s, the US Air Force attempted to increase the range of fixed-wing aircraft by attaching fuel-storage modules to the wingtips. [9] Later, until 1956, the United States Air Force used B-36 bombers to tow two RF-84F camera reconnaissance aircraft with swept wings to achieve the effect of long-range reconnaissance of enemy airspace. After the docking of the reconnaissance aircraft, the two aircraft began to beat violently. After the pilot actively threw out the connection mechanism, the two aircraft successfully separated without serious consequences, but the project was stopped since then [10]. After the 21st century, the concept of combined flight has once again attracted the attention of researchers in various countries, and its application goal has changed to the isomorphic aircraft combination to improve the range and multi-task processing capability. In 2002, Magill and Durham [11] collected data in wind tunnel tests and studied flight modes such as wingtip docking flight, close-range formation flight and towing flight. From 2014 to 2016, Montalvo et al. [12-14] studied aircraft with wingtips connected and end to end connected, and proposed the concept of "meta-aircraft". Based on the lift line method, they found that the short-period mode and Dutch roll mode of the combination varied with the number of connections and connection methods. Kothe and Luckner [15] based on Kane's method and strip theory conducted dynamic modeling and stability analysis of wingtip articulated combined UAV, and found that the flight system with hinged connection was inherently unstable flight mode. In 2018, Cooper and Rothhaar [16] proposed a dynamic model and control scheme for the aerial combination docking process of multiple UAVs based on the wingtip vortex model and the general nonlinear aerodynamic model.

At present, most studies on combined UAVs focus on aerodynamic modeling, flight mechanics analysis and flight control when rectangular wing configuration is connected, while there are relatively few studies on the mechanism of lift-drag characteristics and flow separation characteristics of conformation combination with low aspect ratio, sweep angle and heel ratio for cluster combat. And most of the researches on the aerodynamic modeling of combination are still limited to the simple potential flow theory. In this paper, the effects of the number of connections and the leading edge angle of the wing on the lift-drag and flow separation characteristics of the combination are studied by using high-precision Computational Fluid Dynamics(CFD) numerical calculation method, and the coupling mechanism of the induced drag of the configuration of the low aspect ratio and the pressure difference drag of the wing surface is analyzed.

2. Computational Models and Numerical Simulation Methods

2.1 Calculation Model of UAV with Low Aspect Ratio

The design index of the low aspect ratio UAV is the sea level cruising speed of 20m/s, the weight of the

whole aircraft is 1.5kg, and the design lift coefficient is 0.2. Due to the non-flat tail layout, the wings use the EPPLER 625 anti-bend airfoil. The UAV with low aspect ratio designed in this paper is shown in Figure 1, and the relevant parameters are as follows.

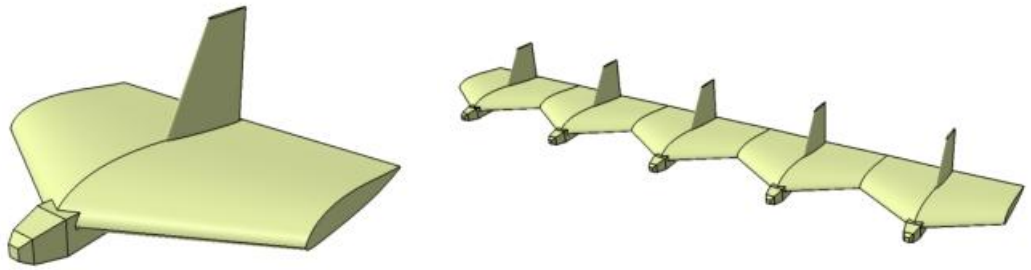

(a) Unit UAV model (b) Combined UAV model

Figure 1-UAV model with low aspect ratio.

Table 1-Related parameters of UAV.

Aspect ratio	1.522	Leading edge sweep angle	30°
Reference area	0.322m^2	angle of Incidence	2°
Wing span	0.7m	Dihedral angle	0
Wing root chord	0.56m	Twist angle	0
Wing tip chord	0.36m	Weight	1.5kg
Airfoil	EPPLER 625	Wing load	4.658kg/m^2

2.2 Numerical Simulation Method and Numerical Example Verification

In order to solve the problem of flow around aircraft under conventional Reynolds number, the fluid domain is discretized by using unstructured polyhedral mesh, and the mesh distribution on the surface of the model is controlled by curvature dimension function. The coupled k-ω Shear Stress Transport (SST) turbulence model [17] was adopted to solve the Reynolds mean Navier-Stokes equation. The Monotone Upstream-Centered Scheme Conversation Laws (MUSCL) format is used for spatial dispersion in numerical calculation. The implicit Lower-Upper Symmetric Gauss-Seidel (LU-SGS) method is used for time discretization and propulsion, and the multi-mesh technique is used to accelerate convergence. The k-ω SST turbulence model is a two-equation mixed model widely used in engineering. The standard k-ε model is used to calculate the pure turbulence region away from the wall, and the Wilcox k-ω model which is suitable for various pressure gradient boundary layer problems is retained in the near-wall region, and the robustness is good.

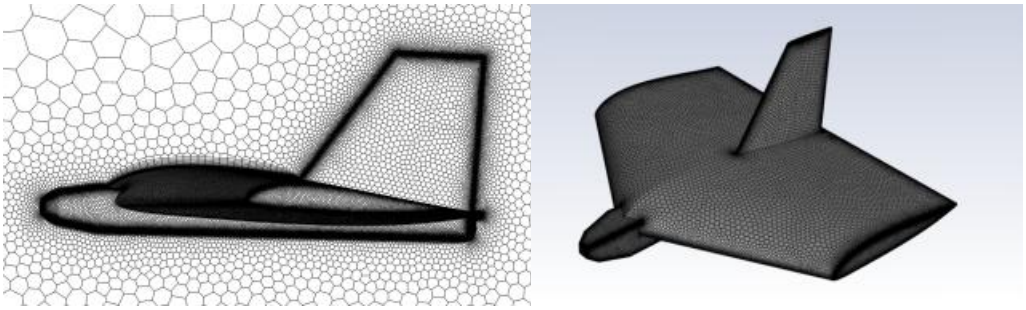

Figure 2-Unit UAV mesh model

In order to verify the accuracy of the calculation method, the ONERA M6 wing of the standard model with abundant aerodynamic test data was selected as the verification object. The distribution of the surface pressure coefficient of the mesh model and 44% wingspan station was shown in Figure 3, and it could be found that the calculated value was in good agreement with the experimental value.

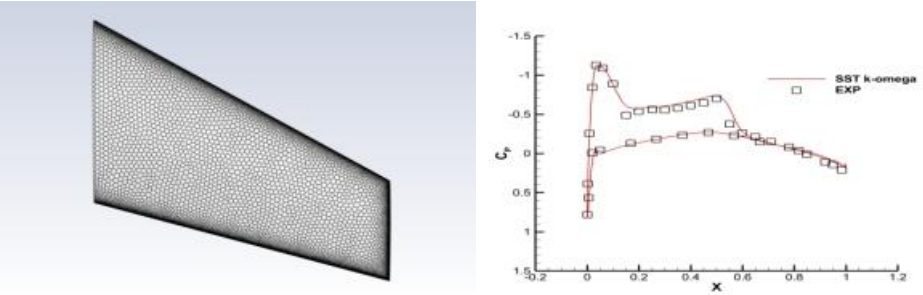

Figure 3-Mesh model and surface pressure coefficient distribution of 44% wingspan stations

3 Calculation Results and Analysis

3.1 Low Aspect Ratio UAV Design

Through CFD numerical calculation, the longitudinal aerodynamic characteristics and lateral and directional static stability curves of a single UAV under cruise state are obtained. It can be seen from Figure 4 that the UAV has a trim angle of attack of 2°, a cruise lift-drag ratio of 8, a stall angle of attack of 24°, a maximum lift coefficient of 1.1, and a stable vertical and horizontal navigation.

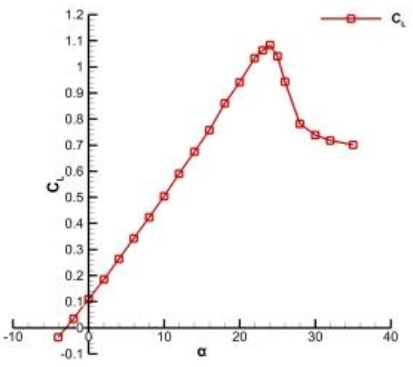

(a) Lift coefficient

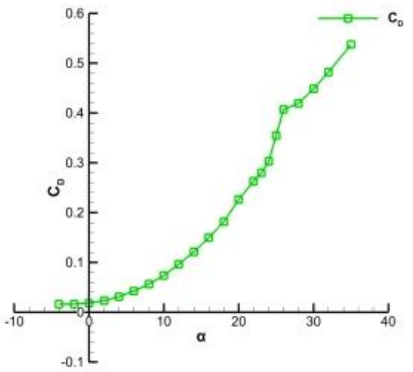

(b) Drag coefficient

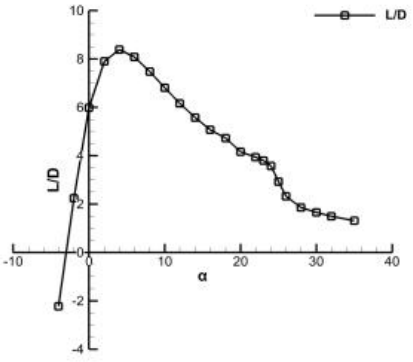

(c) Lift-drag ratio

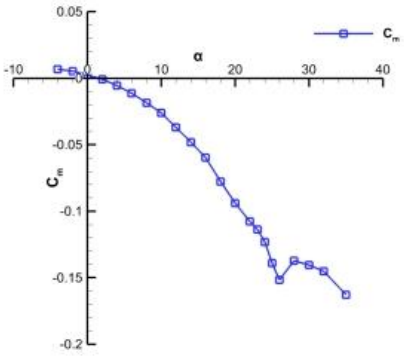

(d) Pitching moment coefficient

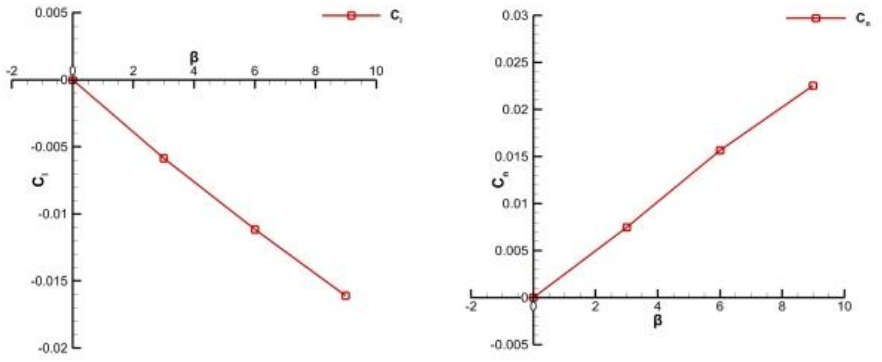

(e) Rolling moment coefficient (f) Yawing moment coefficient

Figure 4-Aerodynamic characteristic curves of UAV with low aspect ratio.

3.2 Aerodynamic characteristics of the combined UAV

The wingtips of the UAV with a low aspect ratio were connected, and the aerodynamic characteristics of the combination in different quantities were calculated by CFD, as shown in Figure 5. It can be found that with the increase of the number of connections, the lift coefficient of the combination in the linear segment (-2°~5°) increases significantly. When two UAVs are connected, the drag coefficient increases, and then gradually decreases with the increase of the number of connections. Only when five UAVs are connected, the drag coefficient of the combination is less than that of the single. At around 6° angle of attack, the increase of the lift coefficient of the combination weakens and has a downward trend. When the number of connections is more than 4, the weakening phenomenon occurs at 5 ° angle of attack. With the increase of the angle of attack, the lift coefficient continues to increase linearly but the slope of the lift line decreases. At this time, the drag coefficient of the combination increases greatly, and the greater the number of connections, the greater the drag coefficient. When five drones are connected, the cruise lift-to-drag ratio increases by about two times, but the increase in lift-to-drag ratio decreases as the number of connections increases. The longitudinal static stability of the combination is enhanced continuously, the trim angle of attack is reduced, the lateral static stability is enhanced first and then weakened, and the weakening is more and more significant, and the hydrostatic stability is basically not affected by the number of connections.

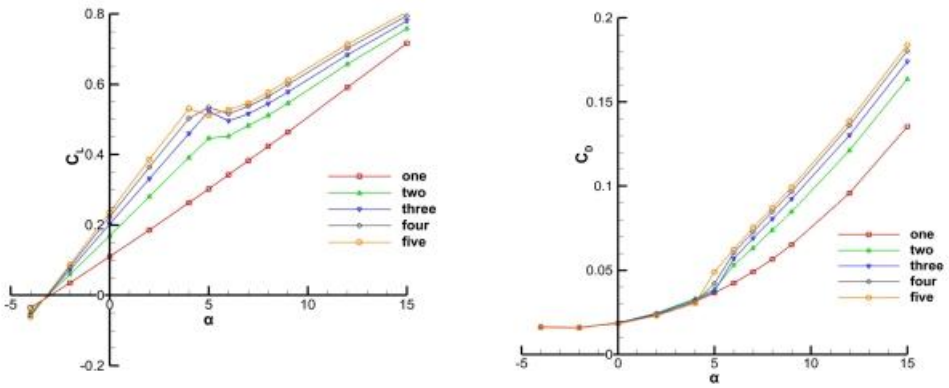

(a) Lift coefficient (b) Drag coefficient

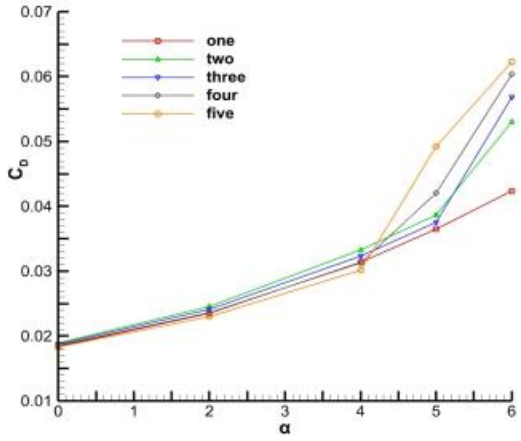

(c) Enlarged figure of linear section of drag coefficient curves。

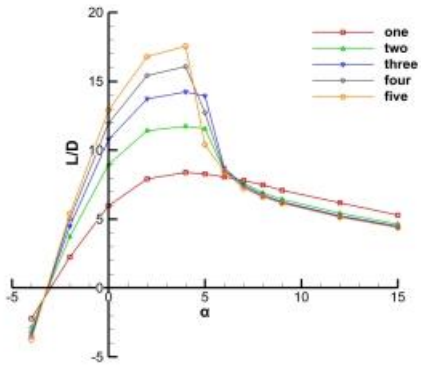

(d) Lift-drag ratio

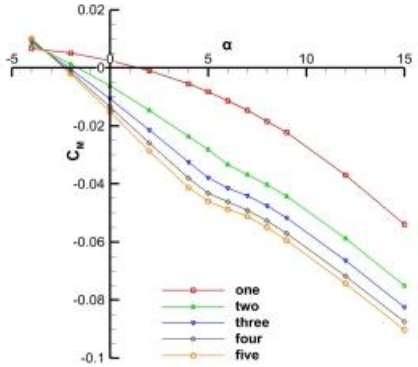

(e) Pitching moment coefficient

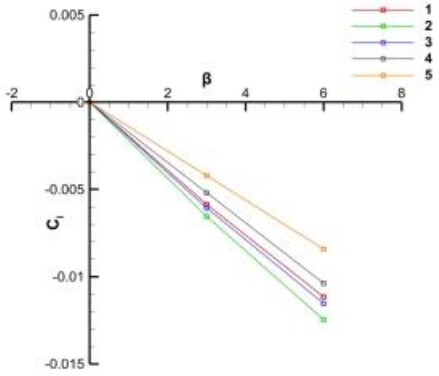

(e) Rolling moment coefficient

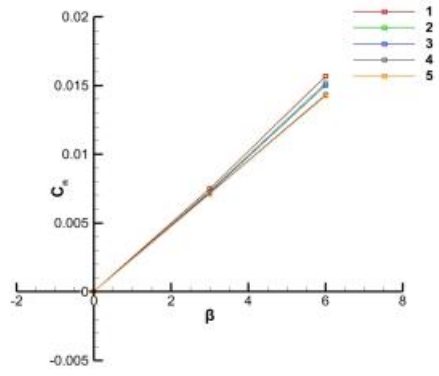

(f) Yawing moment coefficient

Figure 5-Aerodynamic characteristic change curves of combined UAV.

The wingtip connection can reduce the relative wing area affected by the downwash flow generated by the wingtip vortex, thereby increasing the lift and reducing the induced drag. Through calculation, it is found that for the UAV with low aspect ratio, the lift coefficient of the combination increases significantly, but the drag coefficient does not decrease significantly. The drag of UAV is mainly composed of viscous drag, pressure differential drag and induced drag, the latter two kinds of drag are reflected in the pressure distribution of the wing surface. It can be seen from Figure. 6 that with the

increase of the number of connections, the viscous drag coefficient does not change significantly, while the drag generated by the pressure distribution first increases and then decreases, which is consistent with the change of the total drag of the combination. It can be inferred that the increase of pressure differential drag of the combined low aspect ratio UAV cancels out the effect of the wingtip connection on reducing the induced drag. The combined low aspect ratio configuration connection plays the role of drag reduction. It can be seen from Figure. 7 and Figure. 8 that due to the convergence of spanwise flow at the joint, a low pressure area appears at the front edge of the upper wing, while the high pressure area expands at the front edge of the lower wing, which is mainly due to the influence of configuration changes on pressure differential drag. Due to the limited span of the wing, the flow interaction between the upper and lower wing surface of the outer segment forms a wingtip vortex, which increases the pressure of the upper wing surface and decreases the pressure of the lower wing surface, resulting in lower lift and higher drag. For the configuration with low aspect ratio significantly affected by wingtip vortices, the wingtip vortices affect the distribution of the high pressure region near the leading edge of the outer wing, which reduces the range of the high pressure region, resulting in an increase in induced drag and a decrease in pressure differential drag. While the wingtip connection weakens the influence of the wingtip vortex, the high pressure area near the leading edge of the wing on both sides of the connection position is normally distributed, and the induced drag decreases while the pressure difference drag increases. When the number of connections is low, the induced drag does not decrease significantly, and the pressure difference drag increases. The drag coefficient of the combined UAV is greater than that of the unit UAV. Therefore, the coupling effect between the wing surface pressure differential drag and the wingtip vortex induced drag must be considered in the configuration of low aspect ratio. In order to facilitate the analysis, the reasons for the increase of pressure differential drag can be divided into the influence of configuration change on pressure differential drag and the influence of wingtip vortex on pressure differential drag.

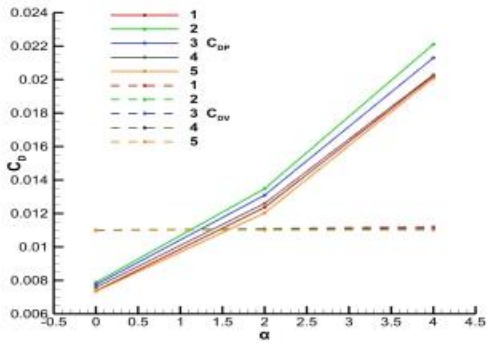

Figure 6-Drag component curves of combined UAV.

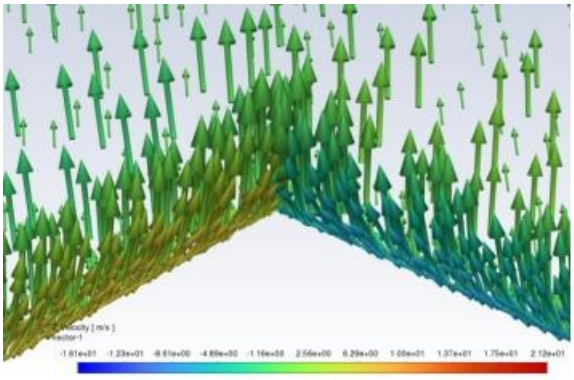

Figure 7- Connection area velocity vector diagram.

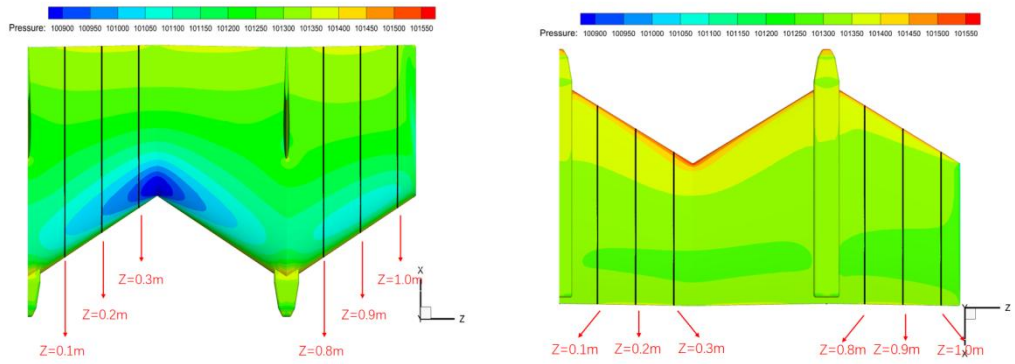

Figure 8-Combined UAV pressure contour at 2° angle of attack .

According to the pressure distribution curves of the six sections in Figure. 9, it can be found that the low-pressure area on the upper wing and the high-pressure area on the lower wing significantly increase the lift force of the wing, while the low-pressure area on the upper wing appears near the position of maximum thickness, which reduces the drag force of the wing to a certain extent, but the high-pressure area on the front edge of the lower wing significantly increases the drag force, showing that the lift coefficient of the combined UAV increases significantly. A phenomenon in which the drag coefficient is not significantly reduced. Due to the sudden change of angle, the convergence speed of spanwise flow at the leading edge of the wingtip connection increases, forming a low pressure area. Moreover, the chord length of the wingtip is the smallest, and the ability to resist the inverse pressure gradient is weak, so the connection position is easy to separate. When the angle of attack reaches about 6°, flow separation occurs on the upper wing surface, the low pressure area on the upper wing surface expands to the rear edge of the wing and interacts with the high pressure area on the lower wing surface, and the pressure on the rear edge of the upper wing surface significantly decreases. At this time, the increase rate of lift decreases and the drag increases significantly. When five UAVs were connected, the combined UAVs separated at 5° angle of attack, and the degree of flow separation gradually increased from both sides to the middle, as shown in Figure 12.

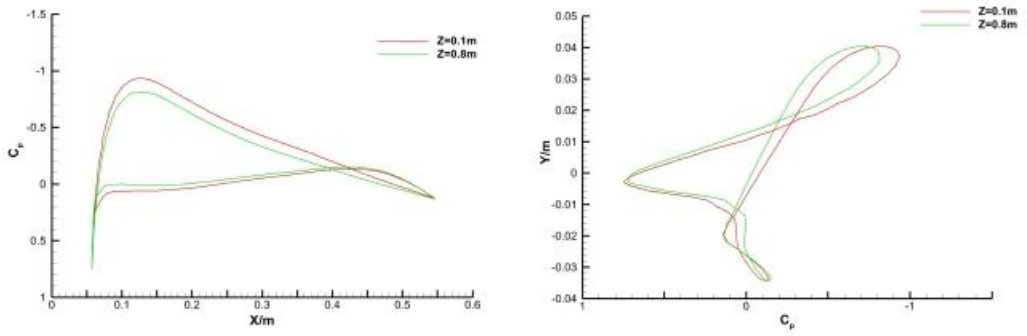

(a) Z=0.1m,Z=0.8m cross section x, y direction pressure coefficient distribution

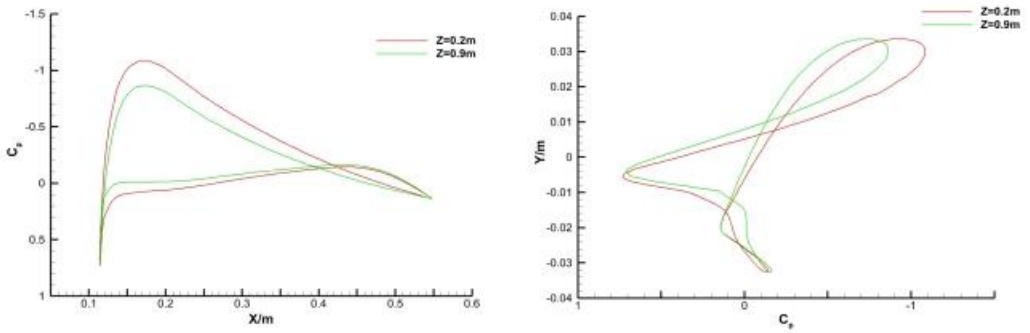

(b) Z=0.2m,Z=0.9m cross section x, y direction pressure coefficient distribution

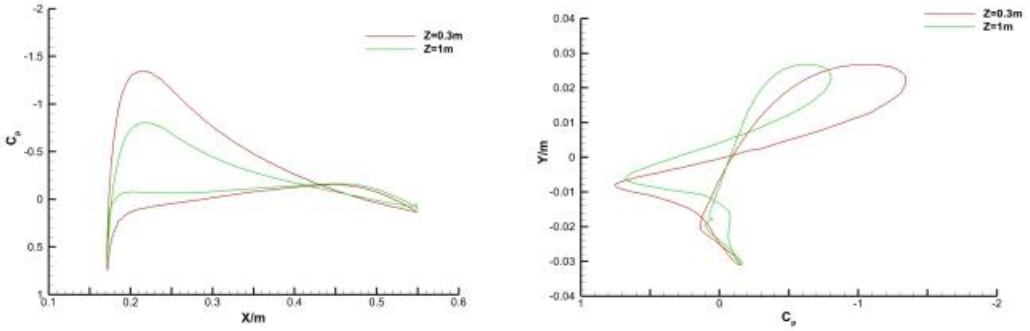

(c) Z=0.3m,Z=1.0m cross section x, y direction pressure coefficient distribution

Figure 9-Comparison curves of pressure distribution in cross section.

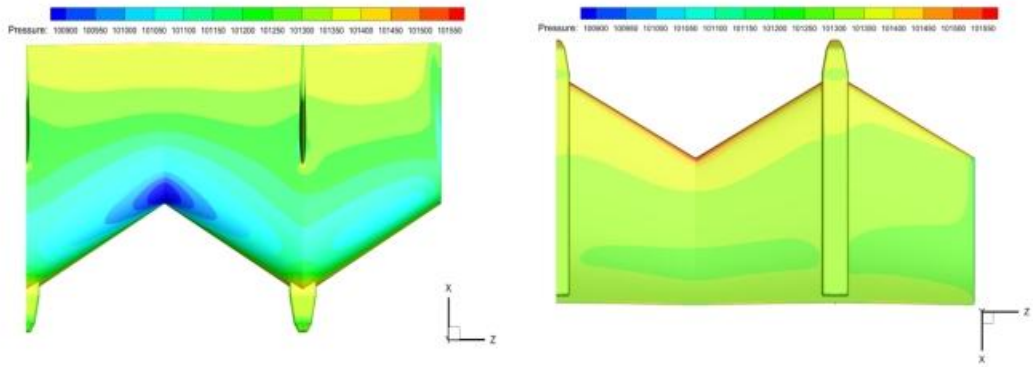

(a) Surface pressure contour of the half model connected by three UAVs at 4° angle of attack

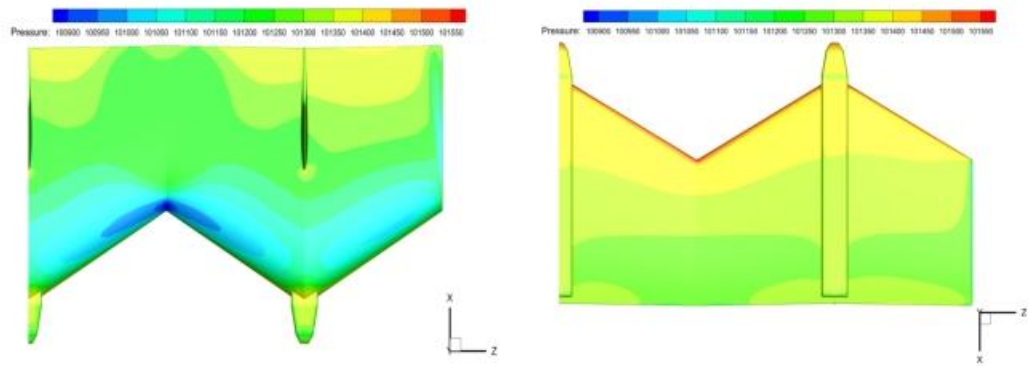

(b) Surface pressure contour of the half model connected by three UAVs at 6° angle of attack

Figure 10-Surface pressure contour connected by three UAVs

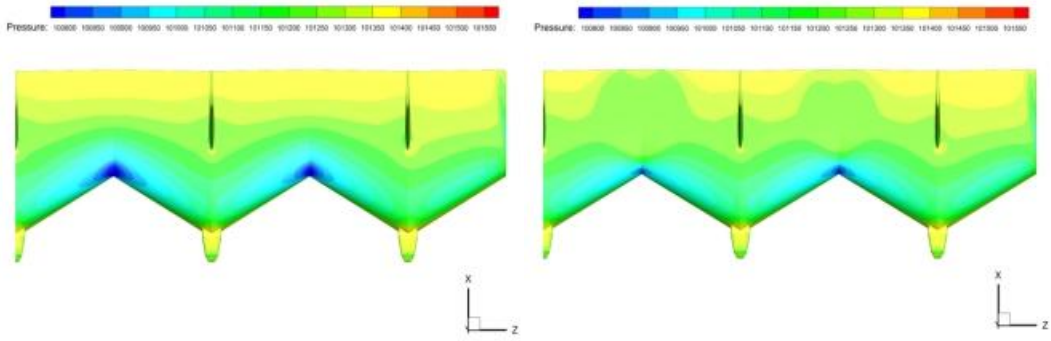

Figure 11-Surface pressure contour connected by three UAVs at 4° and 6° angle of attack

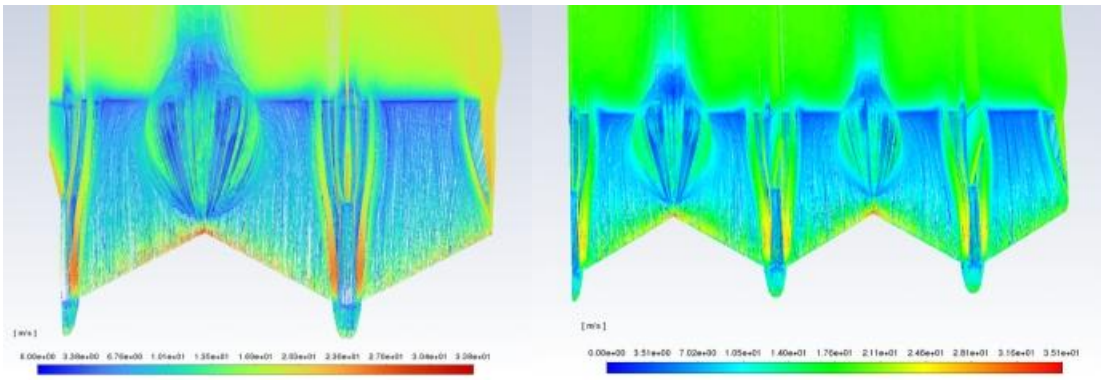

(a) α=6° (b) α=5°

Figure 12- Streamline diagram of combined UAV

3.3 Aerodynamic Characteristics of Each Unit UAV

For the combined UAV, it is necessary to analyze not only the aerodynamic characteristics of the combination, but also the aerodynamic characteristics of each unit of the UAV in the combination, so as to realize the trim of the whole machine, so it is particularly important to analyze the change law of the aerodynamic characteristics of each unit of the UAV.

CFD method was used to calculate the changes in the aerodynamic characteristics of each UAV unit in the combination with different number of connections, as shown in Figure 13. It can be found that when the UAVs are connected, the cruise lift-drag ratio of each unit UAVs is significantly increased. From both sides to the middle, the cruise lift-drag ratio of the unit UAVs increases successively. When four UAVs are connected, the cruise lift-drag ratio of the outermost UAVs has stabilized at about 13 and basically no longer changes. When five UAVs are connected, the cruise lift-drag ratio of the middle UAVs increases to 22, which still has a rising trend. The variation law of the longitudinal static stability margin of each unit UAV is the same as that of the cruise lift-drag ratio. Because the wingtip connection weakens the influence of the downwash airflow of the wingtip vortex, the effective angle of attack of the UAV from outside to inside increases successively. Because the unit UAV is longitudinally static and stable, the bow moment of each UAV from outside to inside under the local angle of attack increases accordingly. The local angle of attack corresponding to the zero-lift pitching moment is not affected by the wingtip connection, so the longitudinal static stability margin of each unit of the UAVs increases from outside to inside. When the number of connections reaches a certain value, the

aerodynamic characteristics of each unit UAV will no longer change with the number of connections, because the influence of downwash airflow generated by wingtip vortices on each unit UAV on the inside can be basically ignored. It is assumed that the influence of a wingtip vortex is a function of the distance between each unit UAV and the wingtip. When infinitely many unit UAVs are connected and the distance between the unit UAVs and the wingtip is greater than a certain value, the influence of the wingtip vortex can be ignored. In this case, the outer unit UAVs are only affected by the corresponding wingtip vortex, and the distance between the outer drone and the wingtip remains unchanged. Therefore, the aerodynamic characteristics of each unit UAV no longer change with the number of connections.

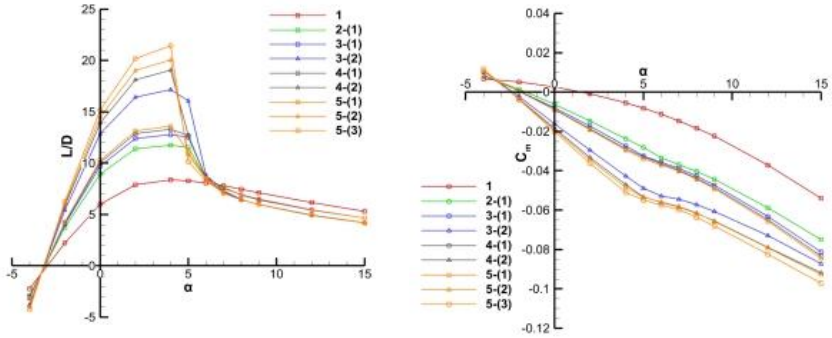

Figure13-Longitudinal characteristic curves of UAVs in each unit of the combination.

4 Optimization Design

4.1 Optimal Design of Angle Sudden Change at Wingtip Joint

Due to the low pressure area at the joint of the converging wingtips of the spanwise flow and the weak drag of the wingtips to the adverse pressure gradient, the lift-drag characteristic of the combination deteriorates significantly at around 6° angle of attack. In order to prevent the combination from stalling at a small angle of attack, the first configuration is optimized for the angle sudden change of the wingtip joint. The first configuration realizes the smooth transition of the wing leading edge angle at the wingtip joint. The second configuration is based on the first by adding a flat wing to reduce the influence of the leading edge spanwise air flow.

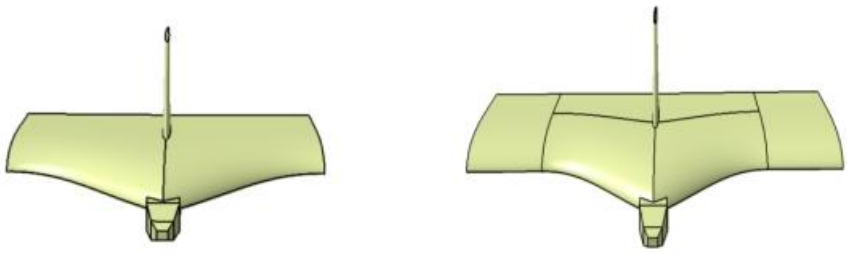

Figure 14-Models of the first and second optimized configurations.

CFD calculation was performed on the unit UAV and combination of the above two configurations respectively, and it was found that the combination of the two configurations still separated at the angle of attack of 7°, and the separation angle lagged only 1°. Therefore, the improvement effect of delayed

separation of the two configurations was not ideal. However, when a straight wing is added, the lift does not decrease, and the drag is reduced due to the increase of the aspect ratio of the single aircraft.

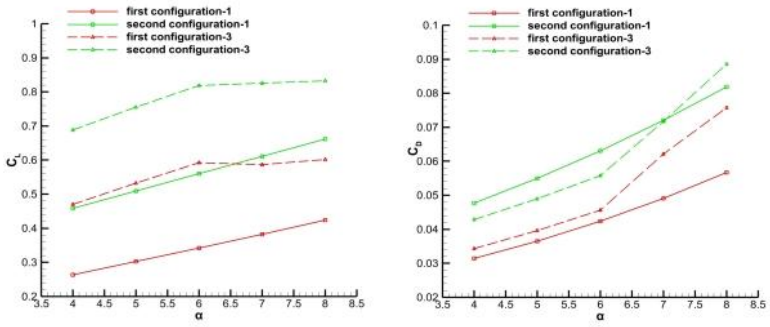

Figure 15-The lift and drag coefficients of the first and second optimized configurations of single UAV and three UAVs.

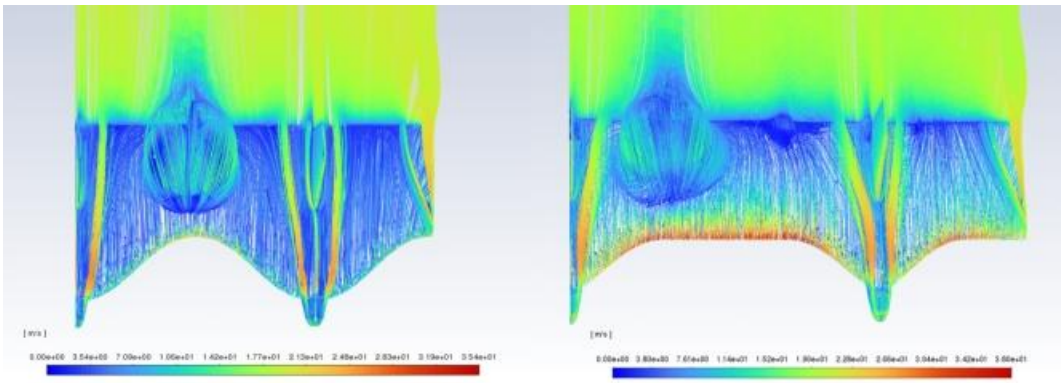

Figure 16-Streamline diagram of the half model connected by three UAVs for the first and second optimized configurations at 7° angle of attack

4.2 Wing Leading Edge Angle Optimization Design

Because the first two configurations can't delay separation effectively, the third configuration uses the flat leading edge of the wing to eliminate the influence of the leading edge spanwise airflow. In the fourth configuration, the forward-swept wing of the leading edge of the wing is used to realize the convergence of the leading edge spanwise flow at the wing root, because the wing root has a strong ability to resist the inverse pressure gradient, so as to delay the occurrence of separation. The third and fourth configurations only change the leading edge angle of the wing, and the other configuration parameters remain unchanged.

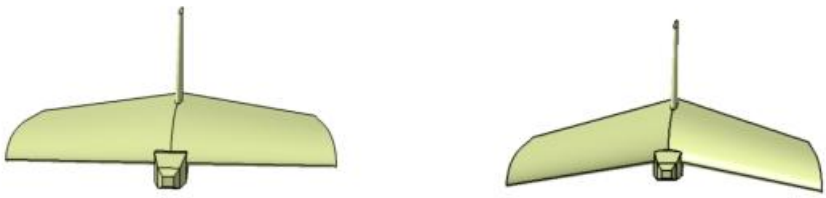

Figure. 17-Models of the third and fourth optimized configurations.

Through CFD calculation, it can be found that the separation of the third and fourth configurations occurs only at 10° angle of attack, and the effect of delaying separation of these two configurations is relatively ideal. The lift coefficient of the flat wing configuration is higher and the drag coefficient of the forward-swept wing configuration is lower, but the drag reduction effect is not achieved in both configurations. This is mainly because the low aspect ratio configuration is significantly affected by the coupling effect of wingtip vortex-induced drag and wing surface pressure differential drag, which will be analyzed in the next section. Moreover, through the pressure distribution on the surface of the third configuration, it can be found that the configuration has a tip ratio, which also leads to the formation of a small range of low pressure areas at the wingtip joint. Because there is no influence of the leading edge sweep angle, the low pressure area at the wingtip joint of the flat wing configuration is weaker than that of the swept wing configuration. Through the pressure distribution on the surface of the forward-swept wing combination, it can be found that the spanwise flow converges at the wing root, while the presence of the fuselage weakens the low pressure area at the wing root to some extent.

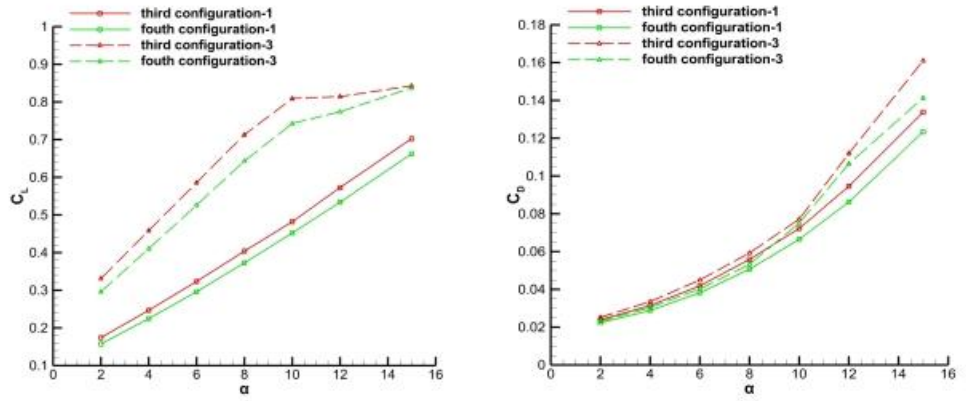

Figure 18. Lift and drag coefficients of the third and fourth optimized configurations of single UAV and three UAVs

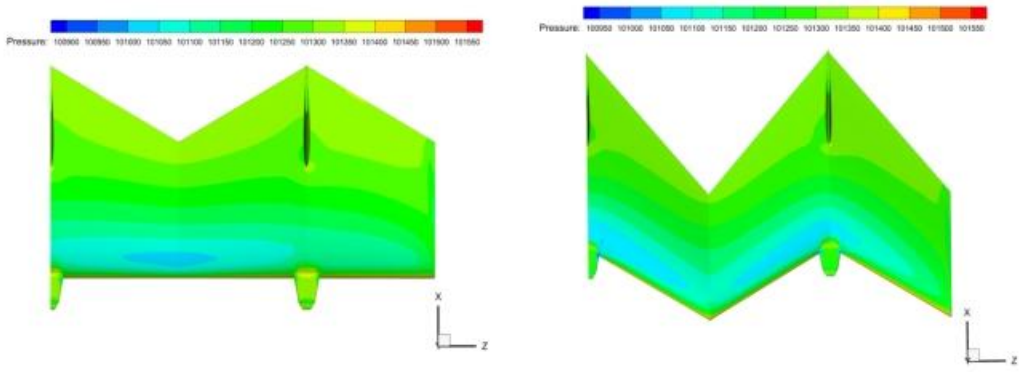

Figure 19- Surface pressure contour of the half model connected by three UAVs for the third and fourth optimized configurations at 2° angle of attack.

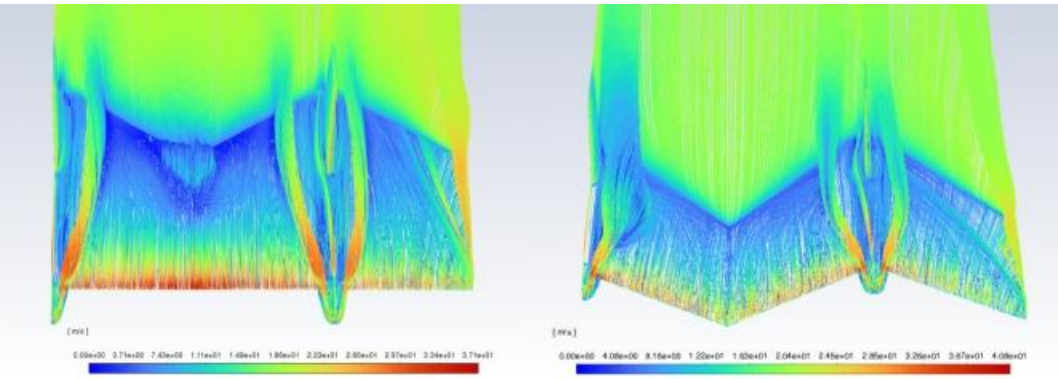

Figure 20- Streamline diagram contour of the half model connected by three UAVs for the third and fourth optimized configurations at 2° angle of attack.

4.3 Analysis of Coupling Effect Between Pressure Differential Drag and Induced Drag

In order to explore the coupling effect between wingtip vortex-induced drag and wing surface pressure differential drag, and ignore the influence of wing contour parameters (leading edge angle, tip ratio) on the surface pressure distribution after the wingtip connection, the fifth configuration, namely rectangular wing configuration, is designed according to the average aerodynamic chord length and wing area of the initial configuration.

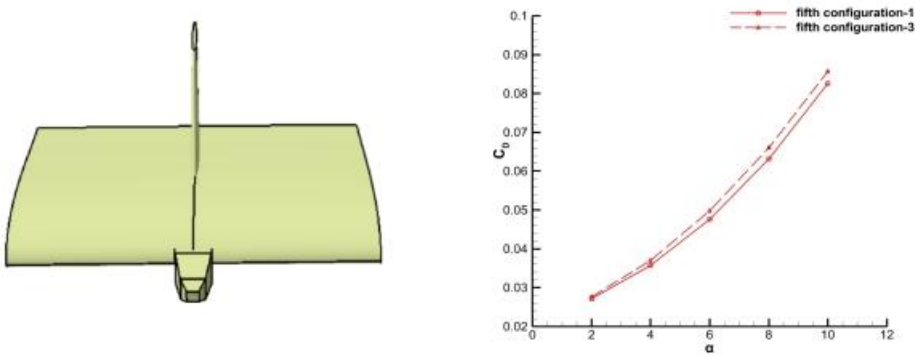

Figure 21-The fifth optimized configuration and the drag coefficient of single-UAV and three-UAVs connection.

Through CFD calculation, it can be found that the drag coefficient increases significantly when three rectangular wings are connected. In order to study the law of the coupling effect of pressure differential drag and induced drag, the type drag of rectangular wing configuration was calculated through the grid model shown in Figure. 23, and then the wing surface of the combination was marked from the outside to the inside, and the variation law of different wing surface drag was analyzed. From the results shown in Figure 24, it can be found that the drag from the outside to the inside wing surface increases at first and then decreases continuously. Because the wing surface of "wingface1-in" is relatively close to the wingtip, while the pressure difference drag increases, the outer wingtip vortex still generates a large induced drag to the wing surface, so the total drag increases. Then the pressure difference drag of the inner wing surface remained basically unchanged, and the induced drag continued to decrease, so the total drag began to decrease.

Because the pressure differential drag and induced drag are reflected in the pressure distribution of the wing surface, they cannot be decomposed. If it is assumed that the pressure difference drag is unchanged and the change of drag is all reflected in the induced drag, quantitative analysis can be carried out. Through calculation, it is found that cruise state type drag accounts for 71.61% of the total drag, and induced drag accounts for 28.39% of the total drag. Theoretically, with the increase of the number of connections, the reduction of total drag can be infinitely close to the proportion of induced drag. As shown in Table 2, when three rectangular wings are connected in configuration, the induced drag on all wing surfaces does not decrease, and the total induced drag increases by 11.80%. When five rectangular wings were connected, the induced drag on the wing surface I was reduced by 22.28% and the total induced drag was reduced by 5.09%.

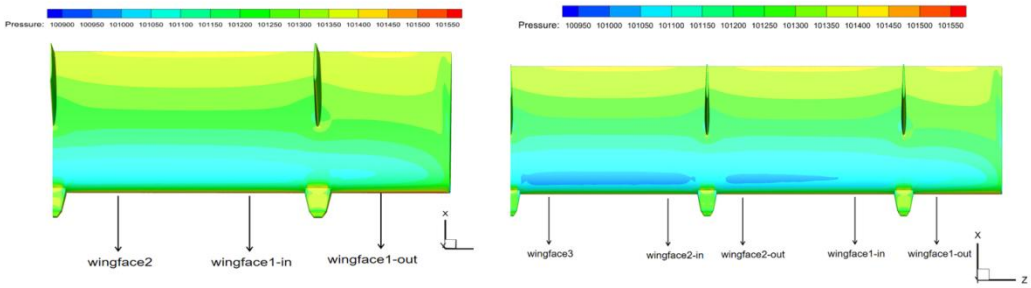

Figure 22-Markings on the wing surface connected by three and five UAVs in the fifth optimized configuration.

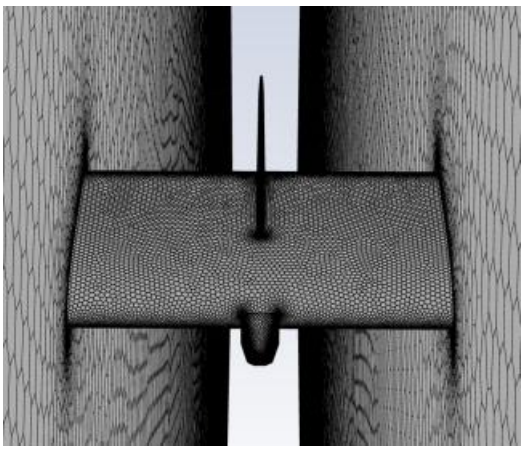

Figure 23-Profile drag calculation mesh model.

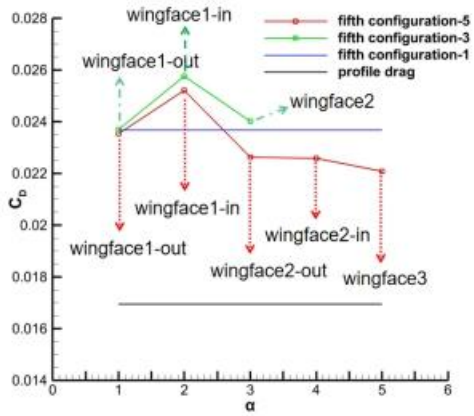

Figure 24-Comparison of wing surface drag coefficient.

Table 2-Data of induced drag coefficient of wing surface.

	3-C_{di}	Rate of increase	Average	5-C_{di}	Rate of increase	Average
Wingface1-out	6.74e-3	0		6.60e-3	0	
Wingface1-in	8.81e-3	30.66%	11.80%	8.26e-3	25.25%	
Wingface2-out	7.06e-3	4.74%		5.68e-3	-13.95%	-5.09%
Wingface2-in				5.64e-3	-14.48%	
Wingface3				5.13e-3	-22.29%	

4.4 Delay Separation Optimization Design Idea

Since the above calculation only considers the flow separation characteristics of the combination when three UAVs are connected, the separation of the third and fourth configuration combinations will certainly advance to a certain extent with the increase of the number of connections. Considering that the downwash flow of the canard wing can effectively inhibit the separation of the forward-swept wing position, and the canard wing configuration has good maneuvering characteristics and high aerodynamic efficiency at low speed [18], it is feasible to apply the canard layout to the combined multi-body UAV to a certain extent, but it needs to be analyzed and verified in many aspects.

Figure 25-Duck type layout combination model

5 Combinatorial Flight Strategy Analysis

Because the combination of flat wing and swept wing with low aspect ratio has better separation delay effect, but the drag reduction effect is not achieved when only three UAVs are connected. In order to develop the flight strategy of the combination which can simultaneously increase lift, reduce drag and delay separation, and compare the different flight strategies, the aerodynamic characteristics of the combination in cruise state when five, seven and nine of the two configurations of the straight wing and the forward-swept wing are connected respectively are calculated and analyzed.

It can be seen from Table 3 and Table 4 that when five straight wing and forward-swept wing configurations are connected, the drag coefficient of the combination is basically the same as that of the single body. When seven or nine wings are connected, the drag coefficient decreases significantly. When the number of connections is the same, the flat wing configuration has higher lift and lift-drag ratio, and the forward-swept wing configuration has lower drag. When nine UAVs were connected, the lift coefficient of the forward-swept wing combination increased by 142.44%, the drag coefficient decreased by 5.12%, and the cruise lift-drag ratio increased by 155.51%. The lift coefficient of the flat wing combination increased by 148.71%, the drag coefficient decreased by 6.34%, and the cruise lift-drag ratio increased by 165.53%. With the increase of the number of connections, the lift drag of the combination is improved, but there are many factors restricting the upper limit of the number of connections. For example, the increase of the number of connections leads to the weakening of the lateral static stability of the combination, and it is also necessary to comprehensively consider the impact of the number of connections on the trim difficulty of the combination, the difficulty of aerial separation of the UAV and the ability to resist sudden separation.

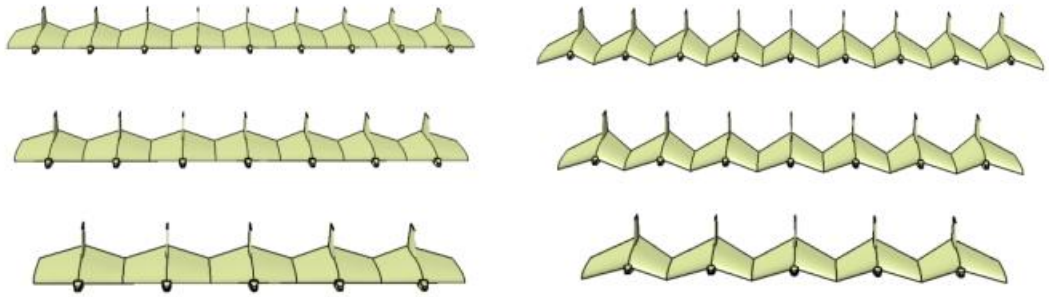

Figure 26–Model of five, seven, nine flat wing and forward-swept wing combinations.

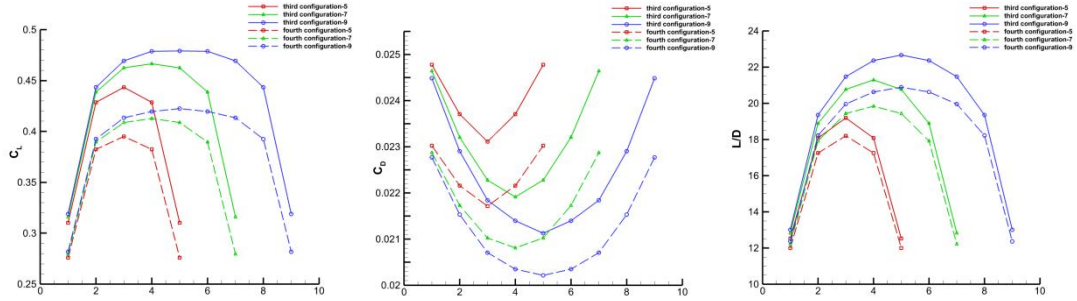

Figure 27-Lift and drag coefficient of each unit UAV of the combination.

Table 3-Lift and drag coefficient of forward-swept wing combination.

Numbers	C_L	Rate of increase	C_D	Rate of increase	L/D	Rate of increase
1	0.1576	0	0.02236	0	7.0474	0
3	0.2967	88.31%	0.02319	3.712%	12.7958	81.57%
5	0.3424	117.27%	0.02242	0.24%	15.2751	116.75%
7	0.3669	132.83%	0.02172	-2.87%	16.8927	139.70%
9	0.3821	142.44%	0.02122	-5.12%	18.0069	155.51%

Table 4-Lift and drag coefficient of flat wing combination.

Numbers	C_L	Rate of increase	C_D	Rate of increase	L/D	Rate of increase
1	0.1742	0	0.02401	0	7.2546	0
3	0.3309	89.98%	0.02517	4.87%	13.1424	81.16%
5	0.3843	120.67%	0.02402	0.037%	16.0026	120.58%
7	0.4144	137.96%	0.02317	-3.50%	17.8889	146.59%
9	0.4332	148.71%	0.02249	-6.34%	19.2634	165.53%

6 Conclusion

In this paper, the effects of the number of connections and the leading edge angle of the wing on the lift drag and flow separation characteristics of the combination were studied by using high-precision CFD

numerical calculation method, and the coupling effects of the configuration induced drag of the low aspect ratio and the wing surface pressure differential drag were analyzed. Conclusions were drawn as follows:

1) The combination layout can effectively improve the lift characteristics of the UAV with low aspect ratio. With the increase of the number of connections, the lift characteristics of the combination will continue to improve. When the wingtips of nine straight wings are connected, the lift coefficient increases by 148.71%. When nine forward-swept wingtips are connected, the lift coefficient increases by 142.44%. Because the low aspect ratio configuration is significantly affected by the coupling effect of the wing surface pressure differential drag and the wingtip vortex induced drag, the drag coefficient of the combination is smaller than that of the single one only when five or more unmanned wingtips with low aspect ratio are connected. When the wingtips of nine straight wings are connected, the drag coefficient decreases by 6.34%. When nine forward-swept wingtips are connected, the drag coefficient decreases by 5.12%.

2) For the low aspect ratio configuration combination, the lift drag characteristics of each unit UAV from the outside to the inside are continuously improved. When nine flat wing configuration wingtips are connected, the lift to drag ratio of the outer unit UAV is increased by 79.46%, and that of the middle unit UAV is increased by 212.58%. When nine forward-swept wing configuration wingtips were connected, the lift to drag ratio of the outer unit UAVs increased by 75.54% and the middle unit UAVs increased by 196.43%.

3) The low aspect ratio configuration combination of swept-back wing has weak drag to separation. When the three planes are connected, flow separation occurs only at 6° angle of attack. The flat wing and forward swept wing have strong drag to separation, and separation occurs at 10° angle of attack when the three planes are connected. With the increase of the number of connections, the aspect ratio of the combination increases, and the ability of resisting separation is gradually weakened. In this paper, a new duck layout combination design concept is proposed to enhance the ability of resisting flow separation of the combination.

Contact Author Email Address

XiaoPing Xu: xuran@nwpu.edu.cn

Acknowledgment

The paper is supported by Natural Science Basic Research Program of Shaanxi(2023-JC-YB-010, 2023-JC-QN-0043), Key Research and Development Program of Shaanxi(2023-YBGY-373).

Copyright Statement

References

[1] JIA Y N, TIAN S Y, LI Q. Recent development of unmanned aerial vehicle swarms[J]. Acta Aeronautica et Astronautica Sinica, 2020, 41(S1): 723738.

[2] NIU Y F, XIAO X J, KE G Y. Operation concept and key techniques of unmanned aerial vehicle swarms[J]. National Defense Science & Technology, 2013, 34(5): 37-43.

[3] AN C, HUO G X, MENG Y, et al. Aerodynamic modeling methods and influence of layout parameters for wingtip-hinged multi-body combined UAV[J]. Acta Aeronautica et Astronautica Sinica, 2024, 45(6): 629587.

[4] ZHOU W, MA P Y, GUO Z. et al. Research of combined fixed wing UAV based on wingtip chained[j]. Acta Aeronautica et Astronautica Sinica, 2022, 43(9): 325946.

[5] YANG Y P, ZHANG Z J, YING P, et al. Flexible modular swarming UAV: Innovative, opportunities, and technical challenges[J]. Flight Dynamics, 2021, 39(2): 1-9, 15.

[6] DU W S, ZHOU Z, BAI Y, et al. Study on multibody dynamics modeling and flight dynamic characteristics of combined aircraft[J]. Acta Armamentarii, 2023,44(8): 2245-2262.

[7] AN C, XIE C C, MENG Y, et al. Flight mechanical analysis and test of unmanned multi-body aircraft[C]//International Forum on Aeroelasticity and Structural Dynamics. 2019:1-17.

[8] ANDERSON C. Dangerous experiments: Wingtip coupling at 15000 Feet[J]. Flight Journal,2000,5（6):64-72.

[9] WRIGHT-PATTERSON A F B. United States Air Force museum guidebook[M]. Ohio: Air Force Museum Foundation, 1975.

[10] NEELY R H. Flutter tests of a 1/25-scale model of the B-36J/RF-84F tip-coupled airplane configuration in the Langley 19-foot pressure tunnel: NACA- RM- SL56A25B [R].Washington, D. C.: Research Memorandum for the U. S. Air Force, 1956.

[11] MAGILL S, DURHAM W. Modeling and simulation of wingtip-docked flight[C]// Proceedings of the AIAA Atmospheric Flight Mechanics Conference and Exhibit. Reston: AIAA,2002.

[12] MONTALVO C. Meta aircraft flight dynamics and controls[D]. Atlanta: Georgia Institute of Technology, 2014.

[13] MONTALVO C, COSTELLO M. Meta aircraft flight dynamics[J]. Journal of Aircraft, 2015, 52(1): 107-115.

[14] TROUB B, MONTALVO C. Meta aircraft controllability[C] // Proceedings of the AIAA Atmospheric Flight Mechanics Conference. Reston: AIAA, 2016.

[15] KÖTHE A, LUCKNER R. Flight mechanical modeling and analysis of multi-body aircraft[C] // International Forum on Aeroelasticity and Structural Dynamics. 2015: 1-12.

[16] COOPER J R, ROTHHAAR P M. Dynamics and control of in-flight wingtip docking[J]. Journal of Guidance, Control, and Dynamics, 2018, 41(11): 2327-2337.

[17] MENTER F R. Two-equation eddy-viscosity turbulence models for engineering applications[J]. AIAA Journal,1994, 32(8): 1598-1605.

[18] MA B F, LIU P Q, Deng X Y. Research advance on a close-coupled canard wing configuration[J] Acta Aerodynamica Sinica, 2003, 21(3): 320-329.